Background-Suppressed Ultrafast Optical Sampling Using Nondegenerate Two-Photon Absorption in a GaAs Photodiode

Paveen Apiratikul, *Student Member, IEEE*, and Thomas E. Murphy, *Senior Member, IEEE*

Abstract—We describe an ultrafast optical sampling system that uses nondegenerate two-photon absorption (2PA) in a GaAs photodiode. By choosing the sampling pulses to have a photon energy below the half-bandgap, we successfully suppress the otherwise large photocurrent associated with 2PA of the strong sampling pulses. Using this approach, we demonstrate a background-suppressed measurement of quasi-4-Tb/s eye diagrams, with temporal resolution that is limited by the sampling pulsewidth.

Index Terms—Nonlinear detection, optical mixers, optical pulse measurements, p-i-n photodiodes, sampling methods, ultrafast optics.

I. INTRODUCTION

O PTICAL sampling systems allow direct monitoring of optical waveforms with a fast temporal resolution. Several techniques have been proposed for optical sampling including coherent mixing [1], sum-frequency generation (SFG) in nonlinear crystals [2], and four-wave mixing (FWM) or cross-phase modulation (XPM) in nonlinear fiber [3], [4] or semiconductor optical amplifiers [5]. The temporal resolution and optical bandwidth of these systems is determined by the combination of the pulsewidth and timing jitter of the sampling pulse, as well as other characteristics of the sampling process such as the walk-off and phase mismatch [6].

Two-photon absorption (2PA) is a nonlinear effect that has an ultrafast response time and very wide optical bandwidth. Compared to other nonlinear processes such as SFG and FWM, 2PA does not require phase matching, and it directly generates a measurable nonlinear photocurrent, thereby eliminating the need for an external optical filter and detector. While 2PA is widely used in time-averaged autocorrelation and cross-correlation measurements [7]–[9], it presents a challenge when there is a disparity between the signal and sampling powers. In sampling applications, the sampling pulse typically has a much higher peak intensity than the signal, and therefore generates a large background photocurrent through degenerate 2PA. This background photocurrent, and the shot-noise associated with it, can easily overwhelm the small mixing signal one seeks to measure. In this
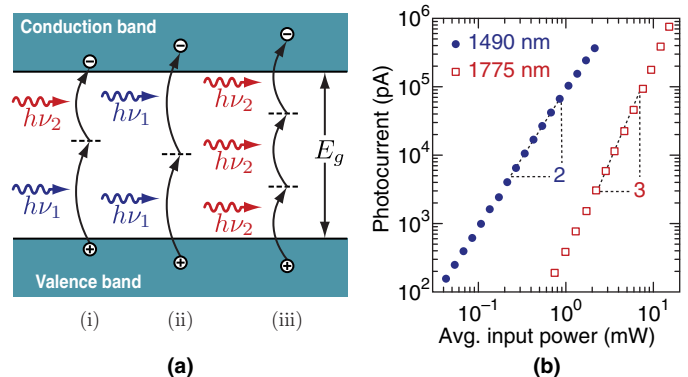
Fig. 1. (a) Three dominant nonlinear processes that contribute to photocurrent: (i) nondegenerate 2PA from sampling and signal pulses; (ii) 2PA from signal pulses; and (iii) 3PA from sampling pulses. (b) The background photocurrent as a function of incident power for $\lambda = 1490$ and 1775 nm.

work, we show that this background photocurrent can be suppressed by using long-wavelength sampling pulses below the half-bandgap of the photodetector. This technique has been recently applied for infrared photon counting [10]. Here we show that nondegenerate 2PA can be used to sample an optical waveform with ultrafast temporal resolution.

II. PRINCIPLE OF NONDEGENERATE 2PA

For the measurements reported here, we used a commercially available 3-GHz GaAs photodiode (Hamamatsu G8522–01), whose bandgap energy allows linear absorption at wavelengths shorter than 870 nm and degenerate 2PA at wavelengths shorter than 1740 nm. The signal and sampling wavelengths were chosen to be $\lambda_1 = 1490$ nm and $\lambda_2 = 1775$ nm, respectively. These wavelengths were chosen to satisfy the following inequalities:

$$2h\nu_2 < E_g < h(\nu_1 + \nu_2) < 2h\nu_1 < 3h\nu_2 \qquad (1)$$

where E_g denotes the bandgap energy of GaAs and ν_1 and ν_2 are the signal and sampling frequencies, respectively. The left-most inequality $2h\nu_2 < E_g$ expresses the important constraint that 2PA of the sampling pulses is prohibited because the sampling photon energy falls below the half-bandgap.

The three expressions appearing to the right of E_g in (1) are each associated with an allowed multiphoton absorption process that can contribute to the measured photocurrent, as depicted in Fig. 1(a). Among these processes, nondegenerate 2PA between the signal and sampling pulses (i) only occurs if the signal and sampling pulses temporally coincide in the detector. Degenerate 2PA of the signal (ii), and three-photon absorption (3PA) of the
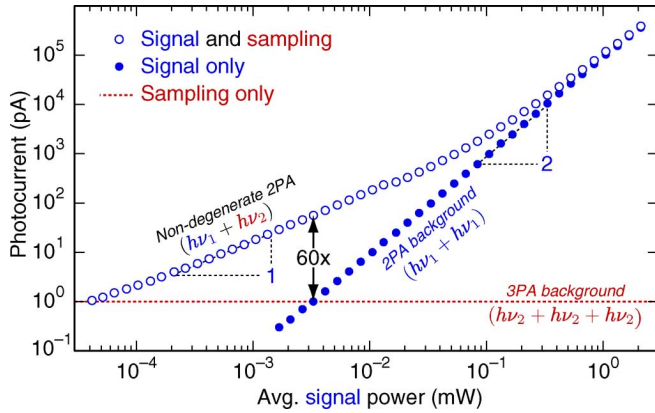
Fig. 2. Measured average photocurrent in GaAs photodiode versus average signal power, for fixed sampling power of 100 μW.
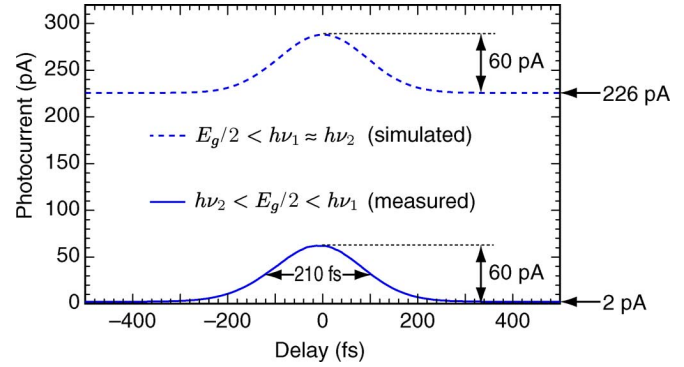

Fig. 3. Cross-correlation between sampling and signal pulses. The solid line represents the measured cross-correlation when $h\nu_2 < E_g/2 < h\nu_1$. The dashed line is the simulated cross-correlation that for the case when $E_g/2 < h\nu_2 \simeq h\nu_1$.

sampling pulses (iii) together constitute a background photocurrent that does not depend on the temporal alignment. These latter two processes are quantified in Fig. 1(b), which shows the measured photocurrent as a function of the average power at wavelengths of 1490 and 1775 nm.

Both the signal and sampling pulses were 150 fs in duration, with a repetition rate of 82 MHz, and were focused to a 3.2-μm spot-size on the surface of the GaAs photodiode using an aspheric lens. The signal pulses at 1490 nm generate a photocurrent through degenerate 2PA, as evidenced by the slope of 2, when plotted on logarithmic axes. The sampling pulses at 1775 nm generate a smaller photocurrent through 3PA, which exhibits a cubic dependence in Fig. 1(b).

For the measurements reported here, the signal and sampling pulse were cogenerated as the signal and idler in a femtosecond optical parametric oscillator, which constrains their wavelengths. Theoretical scaling laws predict that this technique could also work if the signal were tuned to the C-band, with a modest penalty in the nonlinear efficiency [11]. The long wavelength sampling pulses could alternatively be produced using the soliton self-frequency shift in a highly nonlinear polarization-maintaining (PM) fiber [2], [12].

Fig. 2 plots the measured average photocurrent as a function of the average signal power P_1, while the sampling power P_2 was held constant. The sampling pulses had an average power of 100 μW, which, in the absence of signal pulses, generates a background photocurrent of 1 pA due to 3PA, indicated by the dashed line. When the sampling pulses were blocked, the degenerate 2PA photocurrent increases quadratically with the signal power, as expected. When both the sampling and signal pulses were spatially and temporally coincident on the detector, the photocurrent was linearly proportional to the signal power, as indicated by the squares in Fig. 2. For a sampling power of 100 μW, the system achieved a maximum signal-to-background ratio of 60 at a signal power of 3 μW. Despite the large discrepancy between the signal and sampling powers, the system achieves a reasonable dynamic range by suppressing the background 2PA photocurrent of the sampling pulses.

To demonstrate the improved dynamic range, we measured a cross-correlation between the signal and sample pulses by recording the time-averaged photocurrent as a function of the relative delay between the two. The solid curve in Fig. 3 plots

the measured cross-correlation with a signal power of 3 μW and a sampling power of 100 μW. The full-width at half-maximum is measured to be 210 fs, as expected given the signal and sampling pulsewidths of 150 fs. The signal-to-background ratio is measured to be 30 : 1. The background photocurrent of 2 pA is composed of degenerate 2PA of the signal pulses and 3PA of the sampling pulses, each of which generates 1 pA of average photocurrent.

For comparison, we note that if this measurement were performed using a sampling wavelength comparable to the signal wavelength (i.e., both above the half bandgap), then the attainable contrast ratio could never exceed 3 : 1, with the optimal contrast occurring when the signal and sampling pulses have equal power. The dashed curve plotted in Fig. 3 shows the inferred cross-correlation signal that would result if the sampling frequency were tuned above the half-bandgap. When calculating the dashed curve, we reduced the sampling power to 45 μW, to account for the fact that the 2PA coefficient at 1490 nm was measured to be 2.2 $\times$ higher than the coefficient describing nondegenerate 2PA of 1490 and 1775 nm.

While the nondegenerate 2PA signal scales in proportion to $P_1 P_2$, the background photocurrent from 3PA increases as P_2^3 and the degenerate 2PA of the signal grows as P_1^2. Using these scaling relationships, the dynamic range is found to decrease with the sampling power in proportion to $P_2^{-1/2}$. To obtain the highest dynamic range, one should therefore choose the smallest possible sampling power for which the background photocurrents do not exceed the noise floor of the receiver. The dynamic range and detection efficiency can also be improved by using a waveguide-based detector, which benefits from a longer interaction length and smaller mode size. Other semiconductor materials, including III–V alloys, could also be employed to optimize the dynamic range, depending on the signal and sampling wavelengths.

III. ULTRAFAST OPTICAL SAMPLING

Fig. 4 depicts the experimental setup used to demonstrate high-speed optical sampling using nondegenerate 2PA. The setup is similar to that used to measure the cross-correlation, except that the signal pulses were digitally modulated and passively multiplexed to simulate a high-speed time-division-multiplexed channel. The signal pulses were on–off modulated with

82 MS/s (i.e., one measurement per sampling pulse) via offline postprocessing.

Fig. 5 shows measured eye diagrams for three intersymbol spacings of $\tau = 250$, 500, and 750 fs, which would be needed to support aggregate OTDM data rates of 4, 2, and 1.3 Tb/s. These measurements were performed using an average signal power of -2 dBm and a sampling power of $+12$ dBm. Notably, unlike in prior demonstrations, the eye diagrams do not exhibit a large background associated with degenerate 2PA of the pump signal.

IV. CONCLUSION

We demonstrate a high-speed optical sampling system based on nondegenerate 2PA in a GaAs photodetector. By using long-wavelength sampling pulses below the half-bandgap of the detector, we effectively suppress the otherwise large background current that has historically plagued 2PA-based sampling systems. We measure eye diagrams for pseudorandom optical data signals, and show a temporal resolution sufficient for speeds as high as 4 TB/s, limited primarily by the optical pulsewidth.
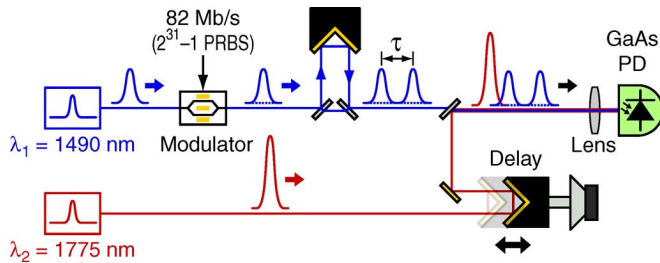

Fig. 4. Experimental setup for optical sampling using on nondegenerate 2PA.
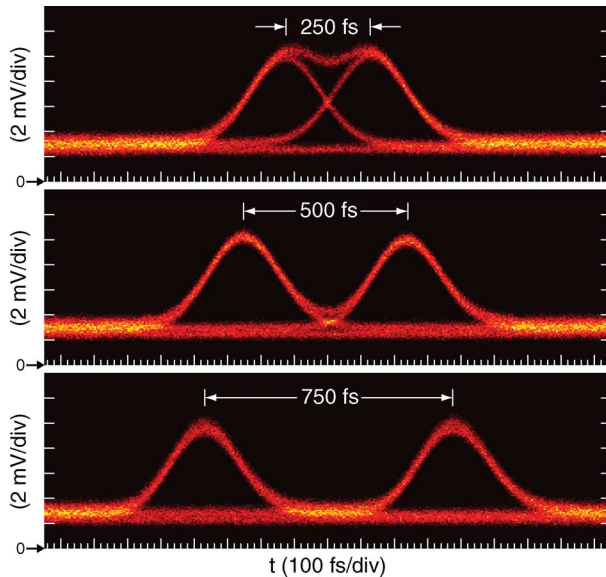

Fig. 5. Measured eye diagram of an on–off keyed signal with intersymbol spacings of 250, 500, and 750 fs.

a $(2^{31} - 1)$ pseudorandom bit sequence (PRBS) in a conventional lithium niobate waveguide electrooptic modulator. The signal pulsewidth broadened to 160 fs as a result of chromatic dispersion in the modulator and fiber pigtails. The resulting 82-Mb/s optical signal was split into two channels, one of which was delayed by $1/82$ μs (i.e., one bit period) in order to produce two uncorrelated tributaries. The two tributaries were recombined after adding an additional relative delay τ to simulate part of a high-speed optical time-division-multiplexed (OTDM) data stream.

As before, the signal and sampling pulses were combined and focused onto the GaAs PIN photodiode. A retroreflector mounted on an audio speaker was used to vary the relative timing between the signal and sampling pulses, while the resulting photocurrent was measured by directly connecting the photodiode to the 50-Ω input channel of a 4-GHz real-time digital oscilloscope. The photodiode has an electrical bandwidth of 3 GHz, which is sufficiently fast to resolve isolated sampling events at 82 MS/s. The oscilloscope waveform was collected at a (free-running) sample rate of 10 GS/s, over a time interval of 1 ms, but the resulting record was down-sampled to

REFERENCES

[1] C. Dorrer, D. C. Kilper, H. R. Stuart, G. Raybon, and M. G. Raymer, "Linear optical sampling," *IEEE Photon. Technol. Lett.*, vol. 15, no. 12, pp. 1746–1748, Dec. 2003.
[2] N. Yamada, S. Nogiwa, and H. Ohta, "640-Gb/s OTDM signal measurement with high-resolution optical sampling system using wavelength-tunable soliton pulses," *IEEE Photon. Technol. Lett.*, vol. 16, no. 4, pp. 1125–1127, Apr. 2004.
[3] J. Li, J. Hansryd, P. O. Hedekvist, P. A. Andrekson, and S. N. Knudsen, "300-Gb/s eye-diagram measurement by optical sampling using fiber-based parametric amplification," *IEEE Photon. Technol. Lett.*, vol. 13, no. 9, pp. 987–989, Sep. 2001.
[4] J. Li, M. Westlund, H. Sunnerud, B.-E. Olsson, M. Karlsson, and P. A. Andrekson, "0.5 Tb/s eye-diagram measurement by optical sampling using XPM-induced wavelength shifting in highly nonlinear fiber," *IEEE Photon. Technol. Lett.*, vol. 16, no. 2, pp. 566–568, Feb. 2004.
[5] C. Schmidt, C. Schubert, S. Watanabe, F. Futami, R. Ludwig, and H. G. Weber, "320 Gb/s all-optical eye diagram sampling using gain-transparent ultrafast-nonlinear interferometer (GT-UNI)," in *Proc. Eur. Conf. Optical Communications (ECOC) 2002*, Copenhagen, Denmark, Paper 2.1.3.
[6] M. Westlund, P. A. Andrekson, H. Sunnerud, J. Hansryd, and J. Li, "High-performance optical-fiber-nonlinearity-based optical waveform monitoring," *J. Lightw. Technol.*, vol. 23, no. 6, pp. 2012–2022, Jun. 2005.
[7] K. Kikuchi, "Optical sampling system at 1.5 μm using two photon absorption in Si avalanche photodiode," *Electron. Lett.*, vol. 34, no. 13, pp. 1354–1355, 1998.
[8] P. J. Maguire, L. P. Barry, T. Krug, M. Lynch, A. L. Bradley, J. F. Donegan, and H. Folliot, "All-optical sampling utilising two-photon absorption in semiconductor microcavity," *Electron. Lett.*, vol. 41, no. 8, pp. 489–490, 2005.
[9] M. Dinu, D. C. Kilper, and H. R. Stuart, "Optical performance monitoring using data stream intensity autocorrelation," *J. Lightw. Technol.*, vol. 24, no. 3, pp. 1194–1202, Mar. 2006.
[10] F. Boitier, J.-B. Dherbecourt, A. Godard, and E. Rosencher, "Infrared quantum counting by nondegenerate two photon conductivity in GaAs," *Appl. Phys. Lett.*, vol. 94, no. 8, p. 081112, 2009.
[11] D. C. Hutchings and E. W. V. Stryland, "Nondegenerate two-photon absorption in zinc blende semiconductors," *J. Opt. Soc. Amer. B*, vol. 9, no. 11, pp. 2065–2074, 1992.
[12] N. Nishizawa, R. Okamura, and T. Goto, "Analysis of widely wavelength tunable femtosecond soliton pulse generation using optical fibers," *Jpn. J. Appl. Phys.*, vol. 38, no. 8, pp. 4768–4771, 1999.